Atlantic Multi-decadal Oscillation Modulates the Relationship Between El Niño-Southern Oscillation and Fire Weather in Australia

Guanyu Liu[1], Jing Li[1], Tong Ying[1]

[1] Department of Atmospheric and Oceanic Sciences, School of Physics, Peking University, Beijing, China, 100871

5   *Correspondence to*: Jing Li (jing-li@pku.edu.cn)

Abstract El Niño–Southern Oscillation (ENSO) is an important driver of fire weather in Australia. The correlation between ENSO and Australian fire weather has strengthened over the recent two decades. However, the causes for this change have not been well investigated. Here, using reanalysis datasets and numerical model simulations, we show that the Atlantic

10   Multi-decadal Oscillation (AMO) could potentially modulate the ENSO-Australian fire weather relationship. The correlation between ENSO and Australia fire weather index (FWI) increases from 0.17 to 0.70 when AMO shifts from its negative phase to its positive phase. This strengthening effect can be explained by the atmospheric teleconnection mechanisms. Specifically, the positive AMO phase, manifested as a warming North and Tropical Atlantic, generates Rossby wave trains and results in high pressures over Australia, which increases local temperature and wind speed but decreases precipitation.

15   This signal superimposes ENSO and thus serves to enhance the ENSO effect on Australian fire weather.

1 Introduction

Australia is the main fire-burning area in the world, as it has more fire-prone lands than the other continents due to the highly flammable biota (Duc et al., 2018). This region frequently suffers from wildfires in austral spring and summer each year (Cai et al., 2009; Dowdy, 2018), especially in the catastrophic 2019/20 wildfire season (Abram et al., 2021; Arriagada et al.,

20   2020). Wildfires in Australia also have a significant impact on the environment (Damany-Pearce et al., 2022; Nguyen et al., 2021), human health (Nguyen et al., 2021; Yu et al., 2020) and ecological systems (Liu et al., 2022). Moreover, as the frequency and intensity of heat waves and droughts in the region increase due to climate warming, wildfires in the region are expected to become more intense, and the related impacts might be more far-reaching (Clarke and Evans, 2018; Jain et al., 2021).

25

As an area with great productivity, wildfire occurrence and spread in Australia are primarily determined by fire weather, so the enhancement of fire weather indicates the increase of fire (Bradstock, 2010; Clarke et al., 2019). Australian fire weather is closely related to the El Niño-Southern Oscillation (ENSO), the leading climate mode controlling key determinants of fire (moisture and temperature variability) (Risbey et al., 2009). In general, El Niño events (the warm phase of ENSO) starve

30 Australia of precipitation and promote long-term droughts and fire weather (Chen et al., 2017; M. Mariani et al., 2016). Moreover, the relationship between ENSO and Australian fire weather has strengthened (Michela Mariani et al., 2018) in the 21st century, but the causes for this strengthening remain unclear. Additionally, the underlying mechanism accounting for this change is poorly understood.

35 Decadal climate variability may also impact fire weather and impose interannual variability. For example, the Atlantic-induced anomalies have a significant impact on Pacific SST and circulation changes (Chikamoto et al., 2016; Chikamoto et al., 2020; Lv et al., 2022), contributing nearly 75% of the tropical SST changes during the satellite era (Li et al., 2016). Markedly, Atlantic decadal variability, i.e., Atlantic Multi-decadal Oscillation (AMO), shifts its phase from negative to positive in the late 1990s. This shift may potentially influence ENSO as well as its teleconnection patterns, including the
40 meteorological conditions in Australia that are closely related to fire weather. In this study, we investigate the Atlantic impact on Australian fire weather and its potential contribution to the ENSO-Australian fire weather relationship. We also attempt to clarify the possible mechanism accounting for this impact. We hope the results can provide insights into the causes of the variability of fire weather in Australia and improve wildfire modeling and forecast in this area.

45 **2 Data and Methods**

2.1 Fire weather index, meteorological data, and climate variability index

Fire occurrence and spread are determined by the confluence of sufficient fuel, an ignition source, and suitable weather, i.e., the fire triangle including heat, fuel, and oxygen (Krawchuk et al., 2009). In areas of high biomass (abundant fuel), such as Australia, fire occurrence over time is primarily modulated by fuel moisture (i.e., weather) and ignitions (lightning and
50 humans) (Bradstock, 2010). The Fire Weather Index (FWI) is a numeric rating of fire intensity that depends on weather conditions and has been shown as an effective indicator of fire danger because it contains both a component of fuel availability (drought conditions) and a measure of the ease of spread (Simpson et al., 2014). Daily FWI (0.25° x 0.25°, 1981-2019) is obtained from the historical data of fire danger indices from the Copernicus Emergency Management Service (Copernicus Contractor, 2021). This dataset provides a complete historical reconstruction of meteorological conditions
55 favorable to the start, spread and sustainability of fires. The daily FWI is then converted to monthly FWI for later analysis.

Meteorological variables, such as surface temperature, precipitation, and wind speed, are critical factors in calculating FWI (Lawson, 2008). Therefore, we primarily use monthly meteorological variables from the re-gridded and interpolated ERA5

reanalysis datasets (Hersbach,2019) from climate data store (CDS) disks to examine responses of meteorological variables to
60   remote SST forcing. According to Lawson (2008), we select 2m temperature (T2M), total precipitation (TP), sea level
pressure (SLP) and 10m wind speed (WND10) from 1981 to 2019, with a resolution of $0.25°\times0.25°$. WND10 is
calculated by the UV component of 10m wind (U10, V10) to represent the intensity of the 10m wind. In order to verify the
robustness of our results, we also used the same variables from the NCEP-NCAR Reanalysis 1 datasets and MERRA-2
datasets (Global Modeling and Assimilation Office, 2015a; Global Modeling and Assimilation Office, 2015b; Kalnay et al.,
65   1996), and re-gridded and interpolated ERA5 reanalysis datasets (Hersbach,2019) from 1959 to 2019. All meteorological
variables were linearly detrended to minimize the impact of global warming on our analysis.

Finally, climate variability indices, such as monthly AMO and Niño 3.4 indices from 1981 to 2019 from the NCAR climate
data guide (Trenberth, 1997; Trenberth and Stepaniak, 2001; Trenberth and Shea, 2006) are used to represent the variability
70   of AMO and ENSO respectively. Moreover, we have explored dataset dependence of the main results by using various SST
datasets, including COBE-SST 2 (COBE), the Met Office Hadley Centre's SST (Hadley), and Kaplan Extended SST v2
(Kaplan), NOAA Extended Reconstruction SST V4 (NOAA V4) and NOAA Extended Reconstruction SST V5 (NOAA V5)
(Huang et al., 2015; Huang et al., 2017; Kaplan et al., 1998; Liu et al., 2015; Rayner et al., 2003). Both the general trends
and variability of AMO and the ENSO-Australian FWI relationship under different AMO phases, as revealed by these
75   datasets, are highly consistent (Figure S1-S2).

Subsequently, we calculated the meteorological variable composite maps of ENSO (AMO). These composite maps are
defined as the meteorological variables of Niño 3.4 (AMO) positive phase years minus those in Niño 3.4 (AMO) negative
phase years. The positive phase year of Niño 3.4 is defined when the absolute value of the moving average of the Niño 3.4
80   index in three months exceeds 0.5 °C for at least five months, and vice versa (Trenberth, 1997).

In addition, simple stochastic variability can drive perceived decadal changes and needs to be considered a potential driver of
variable ENSO behaviors. In order to obtain a more robust conclusion, we estimated all p-values by considering the
autocorrelation using the method by Storch and Zwiers (2000).

85   **2.2 Ocean basin experiments**

To examine the meteorological responses and physical mechanism of the Atlantic impacts on Australia, we performed a
series of ocean basin experiments using the Community Earth System Model-Community Atmosphere Model version 4
(CESM-CAM4) (Gent et al., 2011). The North and Tropical Atlantic Sea Surface Temperature (SST) variabilities were

respectively added to the model to examine the response of meteorological variables in Australia to these remote forcings. Specifically, the monthly SST variability from 1979 to 2015 is added in the North Atlantic region of 25 ° N-75 ° N and the tropical Pacific region of 20 ° N-20 ° S, with a buffer zone of 10 ° added to the north and south of each region. SST forcings over the other regions remain seasonal varying climatological SST. An ensemble simulation with eight members is performed, and the ensemble means are considered the atmospheric response to SST forcing in the target ocean basin. We call this experiment the Ocean Basin Experiments (OBE). These experiments are similar to previous studies (Liu et al., 2022; Wang et al., 2018)

Since the peak season for fire weather in Australia is mainly the local spring (SON, Earl, and Simmonds, 2017), we selected the model responses to SON North Atlantic SST (25°N-65°N, 10°W-60°W) and Tropical Atlantic SST (0-20° N, 10°W-60°W) in the OBE for further analysis.

3 Results

3.1 Influence of AMO on the relationship between ENSO and Australian FWI

As shown in previous studies, Australian fire weather is closely correlated with ENSO (Harris et al., 2014; Mariani et al., 2016). Here, we also found that Australian FWI is significantly positively correlated at $R \approx 0.53$ (p<0.01) with Niño 3.4 index. El Niño events (anomalously positive Niño 3.4 index) induce warmer-than-average temperatures and reduced precipitation across most of Australia in SON. These meteorological anomalies create favorable conditions for igniting and spreading wildfires (Keeley et al., 2022; Littell et al., 2016). In addition to temperature and precipitation, Australia is dominated by a high-pressure center and enhanced northwest winds, which also contribute to wildfires by expanding the burnt area (Clements et al., 2008; Koo et al., 2010).

However, the correlation between ENSO and Australian fire weather is not stable but changes over time. The previous study indicates that the impact of ENSO on Southern Hemisphere fire weather, including in Australia, has become stronger since the start of this century (Mariani et al., 2018). Our analysis also found that the ENSO-Australian FWI correlation increased from 0.34 during 1981-1999 to 0.66 during 2000-2019 (Figure S3 a). However, the other two major southern hemisphere wildfire regions, South Africa and South America, do not show obvious trends (Figure S3 b, c). Mariani et al. (2018) hypothesized that this correlation transition is likely due to global warming. Given that the global warming trend slowed down or even paused between ~2000 and 2015, this hypothesis seems unjustified, motivating us to find other potential causes.

Atmospheric
Chemistry
and Physics
Discussions

Around 2000, a significant global decadal climate variability, the AMO, also transitioned from its negative to its positive

120   phase. Atlantic climate variability has been shown to have a broad impact on the global climate system, including the Pacific Ocean (Chikamoto et al., 2016), the Indian Ocean (Xue et al., 2018), and even the Antarctic (Ren et al., 2022). Indeed, the ENSO-Australian FWI relationship dramatically changed between different AMO phases, with their correlation coefficients increasing from 0.17 to 0.70 between negative and positive AMO phases (Figure 1a), similar to the correlation increase before and after 2000 (Figure S1a) but with a greater contrast. We further calculate a running correlation between ENSO and

125   Australian FWI and compare its time series with that of the AMO (Figure 1b). It is clearly seen that at the negative AMO phase, the ENSO-Australia FWI correlation is low and mostly below 0.3, whereas it increases to above 0.6 or even 0.8 at positive AMO. The time of the transition of the two time series also agrees well, in the late 1990s, although the correlation time series shows a slight lead mainly due to the smoothing treatment.

3.2 Impact of North and Tropical Atlantic on Australian FWI

130   To explain why AMO may reinforce the ENSO-Australian fire weather relationship. It is necessary to examine the impact on Australian meteorological conditions, especially the coherent impact between ENSO and AMO. We approach this question by analyzing reanalysis datasets and OBE simulation results.

As mentioned above, positive ENSO, i.e., El Niño events, corresponds to higher SLP, higher temperature, and lower

135   precipitation, which is conducive to fire generation. For the surface wind, the composite field of the surface wind has the same direction (Southeast wind) as the climatology surface wind, which plays a vital role in strengthening the wind speed and accelerating the expansion of wildfires. This relationship is further corroborated by the composite difference maps of temperature, precipitation, and circulation field between positive and negative Niño 3.4 index conditions

140   We first compare these El Niño-related meteorological responses in Australia during positive (Figure 2d-f) and negative AMO phases (Figure 2g-i) and find that temperature increase and precipitation decrease are both stronger during El Niño when AMO is at its positive phase. The response of SLP and surface winds are even more intense during positive AMO phases compared with the negative phases (Figure 2f & i). Specifically, there might be higher SLP and stronger surface wind during El Niño in the positive phase of AMO. This phenomenon indicates that AMO may potentially enhance the

145   relationship between ENSO and Australian FWI.

We further conduct separate composite analysis of the Australian meteorological fields during positive and negative AMO phases (Figure 2j-l), which appears to show similar patterns to that of ENSO (Figure 2a-c). Specifically, the positive AMO

also corresponds to warmer temperatures and lower precipitation, although the area with significant precipitation changes is

150   mostly concentrated in the southern part. Given that wildfires are also more intense in south Australia (Hennessy et al., 2005), these AMO-associated meteorological anomalies thus also serve to enhance fire weather. Positive AMO also corresponds to the easterly anomaly wind in eastern Australia. Due to the topography of the Great Watershed in eastern Australia, the easterly wind adiabatically sinks, increasing temperature and reducing humidity, resulting in a high temperature and low humidity environment over this biomass-rich area (Kriwoken, 1996). These similarities suggest that positive AMO may

155   reinforce the ENSO effect on Australian FWI and result in more severe and extensive wildfires. We also examined the differences in the ENSO events between the two periods with different AMO phases (1981-1999 and 2000-2019, Figure S4), but found no significant difference in their spatial patterns (Figure S4e & f), indicating that ENSO flavor is an unlikely factor for the shifted ENSO-Australian FWI relationship.

160   Because reanalysis datasets contain many different physical processes, to isolate the AMO effect, we continue to examine the responses of major meteorological variables (T2M, TP, SLP, U10, V10) to North and Tropical Atlantic in the OBE. The detrended and normalized SON meteorological variables are regressed on the detrended and normalized SON Tropical Atlantic and North Atlantic SST in OBE. The regression coefficients, representing the responses of local meteorological variables to remote SST forcings in the corresponding ocean basin, are shown in Figure 3.

165

For the Tropical Atlantic, the anomalously high SST in this region corresponds to higher T2M and lower TP in southern Australia (Figure 3a-b), the primary wildfire regime. This anomaly also corresponds to anomalously easterly and northerly winds in eastern Australia (Figure 3c). These winds will sink due to topographic factors, increasing temperature, and reduced humidity. These meteorological anomalies may reduce moisture in combustible plants and increase surface dryness, creating

170   favorable conditions for igniting and spreading wildfires. Similarly, although the responses of these meteorological variables are relatively weaker to the North Atlantic forcing (Figure 3d-f), their change directions agree with those under the Tropical Atlantic forcing, i.e., positive North Atlantic SST anomalies correspond to higher T2M and less TP in southern Australia. Therefore, the impact from tropical Atlantic appears stronger and more significant. Nonetheless, the impact of North Atlantic on precipitation is statistically significant across southern and western Australia and cannot be ignored.

175

The consistent results in reanalysis (Figure 2) and OBE (Figure 3) indicate that the positive AMO phase, associated with warm North and Tropical Atlantic SST anomalies, induces warmer and drier weather in Australia, especially in the southern part. This inducing reinforces the positive ENSO signal on Australian fire weather, thus enhancing the ENSO-fire weather relationship there. In addition, the modulation effect of AMO on Australian climate is also significant in different periods

180 (1981-2019 and 1959-2019) and different reanalysis data sets (ERA5, NCEP-NCAR, and MERRA-2), which further confirms the robustness of our findings (Figure S5-S7).

3.3 Possible mechanism accounting for this modulation

To clarify the physical process that the Atlantic impacts on Australia, we examine the responses of the 500 hPa geopotential height (GPH) responses in the North and Tropical Atlantic OBE and the mechanisms by which North Atlantic and the

185 Tropical Atlantic respectively affect Australian FWI. Following Sardeshmukh and Hoskins (1988), the dynamics of Rossby waves can be diagnosed by analyzing the barotropic vorticity equation at 200 hPa. Specifically, we diagnosed the dynamics of Rossby waves by analyzing the barotropic vorticity equation at 200 hPa, i.e., the Rossby wave source (RWS) that quantifies vorticity forcing associated with low-level convergence and upper-level divergence.

190 For Tropical Atlantic, the thermal forcing in the tropical Atlantic drives changes to the zonal Walker circulation. This change may lead to upward vertical motion and local convection over the Atlantic, whereby the corresponding low-level convergence and upper-level divergence subsequently produce an intensification of the local Hadley circulation (Li et al., 2014; Li et al., 2015). In doing so, upper-level convergence is enhanced at the descending branch of the Hadley cell (Simpkins et al., 2014). This enhancement consequently intensifies the local Hadley circulation and becomes a vital source

195 of Rossby waves that propagate eastward with the climatological mean flow in the Southern Hemisphere (Figure 4c). This Rossby wave source is clear over the South Atlantic (Figure 4c), and the corresponding Rossby wave will consequently propagate to Australia and intensify the high pressure there (Figure 4a). In summary, anomalous deep convection in response to increased SSTs in Tropical Atlantic drives anomalous divergence of the large-scale flow that extends away from the local heating by modulating the Hadley and Walker circulations. This process has been discussed in detail by Simpkins et al.

200 (2014).

For North Atlantic, the warmer Atlantic heats the air above, thus forming a local high-pressure center in the upper troposphere. This signal generates the Rossby wave source over the North Atlantic (Figure 4d). The corresponding Rossby wave train will propagate from the west to the east with alternating high and lower pressure centers, which arrive in

205 Australia as a high-pressure anomaly (Figure 4b and 4d). This high pressure corresponds to descending motions over Australia with drier and hotter air, unfavorable to cloud and rain formation. The southward propagation of Rossby waves originating from the Atlantic is also supported by previous works (Miller et al., 2007; Zhao et al., 2019), which form the basis of the teleconnection between the North Atlantic and Australia. Previous studies also indicate that the AMO can modulate ENSO effects by the similar Rossby wave dynamics (Lin and Li, 2012; Nagaraju et al., 2018).

210 **4 Conclusions**

Fire weather in Australia is closely related to the variability of ENSO. The correlation between them has been strengthened in the recent two decades, yet the cause has not been fully clarified. By analyzing reanalysis datasets and conducting ocean basin experiments using a global climate model, our study offers a plausible explanation that the AMO modulates the ENSO-Australian fire weather relationship. The correlation coefficient between ENSO and the Australian Fire Weather

215 Index (FWI) increases from 0.17 to 0.70 when AMO transitions from negative to possible phases. Under positive AMO, El Niño conditions correspond to stronger temperature increase, precipitation decrease, stronger surface winds favorable for wildfire generation, and vice versa. Physically, positive AMO, associated with warmer North and Tropical Atlantic SST, forms a local low-pressure center, which propagates to the southwest as a Rossby wave train. This wave train arrives in Australia as a higher-pressure anomaly, inducing descending air and leading to warmer and drier meteorological conditions

220 conducive to wildfire generation. These meteorological anomalies superimpose the positive ENSO-induced meteorological changes and enhance the response of Australian fire weather to ENSO. Previous studies also point out that the positive AMO, characterized by the basin-wide Atlantic warming, induces an Atlantic-Pacific sea surface temperature seesaw, strengthening the Walker circulation over the Pacific (Chafik et al., 2016; McGregor et al., 2014; Wang et al., 2013). This strengthened Walker circulation might also amplify ENSO's effects on Australian FWI.

225

Compared with previous studies, this work sheds light on the teleconnection between AMO and Australian climate and fire weather on the decadal scale. The Australian mega-fire in the austral spring of 2019 has been attributed to the El Niño event, positive southern annular mode, and the positive Indian Ocean Dipole event of the year (Abram et al., 2021; Nolan et al., 2020; van Oldenborgh et al., 2021). Our study reveals that this year also corresponds to higher than normal Atlantic SST

230 (Figure S8), which may strengthen the Australian atmospheric response to the El Niño event, further leading to prolonged dry seasons and increased heat waves. Admittedly, the Pacific decadal variability (such as the Pacific Decadal Oscillation) also plays an essential role in Australia's climate (Power et al., 1999). However, previous research indicates that the Pacific variability may be at least partly triggered by that of the Atlantic (Li et al., 2016; Ren et al., 2021), highlighting the vital role of the latter in the Earth's climate system. Note that another major decadal climate variability, the Interdecadal Pacific

235 Oscillation (IPO), also changed its phase in the late 1990s. We also investigated its modulation effect on ENSO and Australian FWI but found it not as significant as that of AMO in both observation and simulation (Figures not shown). In the future, we plan to investigate the impact of other ocean basins on Australian fire weather and the ENSO-Australian fire weather relationship in the future.

240 **Data availability**

Atmospheric
Chemistry
and Physics
Discussions

The history Fire Weather Index (FWI) data is downloaded from fire danger indices historical data in Copernicus Emergency Service (https://doi.org/10.24381/cds.0e89c522). The meteorological reanalysis data is downloaded from ERA5 monthly averaged data in the climate data store (CDS) (https://doi.org/10.24381/cds.adbb2d47). The NCEP-NCAR Reanalysis 1 data is downloaded from Physical Sciences Library (https://psl.noaa.gov/data/gridded/data.ncep.reanalysis.html). The MERRA-2

245 data is downloaded from MDISC (https://disc.gsfc.nasa.gov/datasets/M2TMNXFLX_5.12.4/summary?keywords=MERRA2_100.tavgM_2d_flx_Nx and https://disc.gsfc.nasa.gov/datasets/M2TMNXSLV_5.12.4/summary?keywords=MERRA2_100.tavgM_2d_slv_Nx). AMO and Niño 3.4 indexes are obtained from the NCAR climate data guide for the AMO index (https://climatedataguide.ucar.edu/climate-data/atlantic-multi-decadal-oscillation-amo) and Niño 3.4 index

250 (https://climatedataguide.ucar.edu/climate-data/nino-sst-indices-nino-12-3-34-4-oni-and-tni), respectively. The sea surface temperature data is obtained from NOAA Extended Reconstructed Sea Surface Temperature (SST) V4 (https://psl.noaa.gov/data/gridded/data.noaa.ersst.v4.html) NOAA Extended Reconstructed Sea Surface Temperature (SST) V5 (https://psl.noaa.gov/data/gridded/data.noaa.ersst.v5.html) COBE-SST 2 (https://psl.noaa.gov/data/gridded/data.cobe2.html), HadISST (https://www.metoffice.gov.uk/hadobs/hadisst/), and Kaplan

255 Extended SST V2 (https://psl.noaa.gov/data/gridded/data.kaplan_sst.html).

Author contributions

The paper was written by GY and JL and designed by JL. The data analysis was performed by GY and TY. All the co-authors contributed to the interpretation of results and the improvement of this paper.

260

Competing interests

The contact author has declared that neither they nor their co-authors have any competing interests.

Disclaimer

265 Publisher's note: Copernicus Publications remains neutral with regard to jurisdictional claims in published maps and institutional affiliations.

Acknowledgement

Financial support

References

275

Abram, N.J., Henley, B.J., Sen Gupta, A. et al.: Connections of climate change and variability to large and extreme forest fires in southeast Australia, Communications Earth & Environment, 2, 8, https://doi.org/10.1038/s43247-020-00065-8, 2021.

Arriagada, N. B., Palmer, A. J., Bowman, D., Morgan, G. G., Jalaludin, B. B., and Johnston, F. H.: Unprecedented smoke-related health burden associated with the 2019-20 bushfires in eastern Australia, Med. J. Aust., 213, 282-283,

280 https://doi.org/10.5694/mja2.50545, 2020.

Bradstock, R. A.: A biogeographic model of fire regimes in Australia: current and future implications, Glob. Ecol. Biogeogr., 19(2), 145-158, https://doi.org/10.1111/j.1466-8238.2009.00512.x, 2010.

Cai, W., Cowan, T., and Raupach, M.: Positive Indian Ocean Dipole events precondition southeast Australia bushfires, Geophys. Res. Lett., 36, L19710. https://doi.org/10.1029/2009GL039902, 2009.

285 Chafik, L., Hakkinen, S., England, M. H., Carton, J. A., Nigam, S., Ruiz-Barradas, A., Hannachi, A., and Miller, L.: Global linkages originating from decadal oceanic variability in the subpolar North Atlantic, Geophys. Res. Lett., 43(20), 10909-10919. https://doi.org/10.1002/2016GL071134, 2016.

Chen, Y., Morton, D. C., Andela, N., van der Werf, G. R., Giglio, L., and Randerson, J. T.: A pan-tropical cascade of fire driven by El Nino/Southern Oscillation, Nat. Clim. Change, 7(12), 906-911, https://doi.org/10.1038/s41558-017-0014-8,

290 2017.

Chikamoto, Y., Mochizuki, T., Timmermann, A., Kimoto, M., and Watanabe, M.: Potential tropical Atlantic impacts on Pacific decadal climate trends, Geophys. Res. Lett., 43(13), 7143-7151, https://doi.org/10.1002/2016GL069544, 2016.

Chikamoto, Y., Johnson, Z. F., Wang, S. Y. S., McPhaden, M. J., and Mochizuki, T.: El Nino-Southern Oscillation Evolution Modulated by Atlantic Forcing, J. Geophys. Res. Oceans, 125(8), e2020JC016318,

295 https://doi.org/10.1029/2020JC016318, 2020.

Clarke, H., and Evans, J. P.: Exploring the future change space for fire weather in southeast Australia, Theor. Appl., 136, 513-527, https://doi.org/10.1007/s00704-018-2507-4, 2019.

Clarke, H., Gibson, R., Cirulis, B., Bradstock, R. A., and Penman, T. D.: Developing and testing models of the drivers of anthropogenic and lightning-caused wildfire ignitions in south-eastern Australia. J. Environ. Manage., 235, 34-41,

300 https://doi.org/10.1016/j.jenvman.2019.01.055, 2019.

Clements, C. B., Zhong, S. Y., Bian, X. D., Heilman, W. E., and Byun, D. W.: First observations of turbulence generated by grass fires, J. Geophys. Res. Atmos., 113, D22102, https://doi.org/10.1029/2008JD010014, 2008.

Copernicus Contractor: Fire danger indices historical data from the Copernicus Emergency Management Service [Data set], Zenodo, https://doi.org/10.5281/zenodo.5754302, 2021.

305 Damany-Pearce, L., Johnson, B., Wells, A. et al.: Australian wildfires cause the largest stratospheric warming since Pinatubo and extends the lifetime of the Antarctic ozone hole, Sci. Rep., 12, 12665, https://doi.org/10.1038/s41598-022-15794-3, 2022.

Dowdy, A. J.: Climatological Variability of Fire Weather in Australia. J. Appl. Meteorol. Climatol., 57(2), 221-234. https://doi.org/10.1175/JAMC-D-17-0167.1, 2018.

310 Duc, H. N., Chang, L. T. C., Azzi, M., and Jiang, N. B. : Smoke aerosols dispersion and transport from the 2013 New South Wales (Australia) bushfires. Environ. Monit. Assess, 190(7), 428, https://doi.org/10.1007/s10661-018-6810-4, 2018.

Earl, N., and Simmonds, I.: Variability, trends, and drivers of regional fluctuations in Australian fire activity. J. Geophys. Res. Atmos., 122(14), 7445-7460, https://doi.org/10.1002/2016JD026312, 2017.

Gent, P. R., Danabasoglu, G., Donner, L. J., Holland, M. M., Hunke, E. C., Jayne, S. R., Lawrence, D. M., Neale, R. B.,

315 Rasch, P. J., Vertenstein, M., Worley, P. H., Yang, Z., and Zhang, M.: The Community Climate System Model Version 4. J. Clim., 24(19), 4973-4991, https://doi.org/10.1175/2011JCLI4083.1, 2011.

Global Modeling and Assimilation Office (GMAO): MERRA-2 tavgM_2d_flx_Nx: 2d,Monthly mean, Time-Averaged,Single-Level,Assimilation,Surface Flux Diagnostics V5.12.4, Greenbelt, MD, USA, Goddard Earth Sciences Data and Information Services Center (GES DISC), Accessed: [Acceesed on 2022-11-

320 10], https://doi.org/10.5067/0JRLVL8YV2Y4, 2015a.

Global Modeling and Assimilation Office (GMAO): MERRA-2 tavgM_2d_slv_Nx: 2d,Monthly mean, Time-Averaged,Single-Level,Assimilation,Single-Level Diagnostics V5.12.4, Greenbelt, MD, USA, Goddard Earth Sciences Data and Information Services Center (GES DISC), Accessed: [Acceesed on 2022-11-10], https://doi.org/10.5067/AP1B0BA5PD2K, 2015b.

325   Harris, S., Nicholls, N., and Tapper, N.: Forecasting fire activity in Victoria, Australia, using antecedent climate variables
         and ENSO indices. International Journal of Wildland Fire, 23(2), 173-184. https://doi.org/10.1071/WF13024, 2014.
         Hennessy, K. J., Lucas, C., Nicholls, N., Bathols, J., Suppiah, R., and Ricketts, J. H.: Climate change impacts on fire-weather
         in south-east Australia. 88 pp, 2005.
         Hersbach, H., Bell, B., Berrisford, P., Biavati, G., Horányi, A., Muñoz Sabater, J., Nicolas, J., Peubey, C., Radu, R., Rozum,
330   I., Schepers, D., Simmons, A., Soci, C., Dee, D. and Thépaut, J-N.: ERA5 monthly averaged data on single levels from 1979
         to present. Copernicus Climate Change Service (C3S) Climate Data Store (CDS). [Accessed on 2022-05-23],
         https://doi.org/10.24381/cds.f17050d7, 2019.
         Huang Boyin, F. Banzon Viva, Freeman Eric, Lawrimore Jay, Liu Wei, C. Peterson Thomas, M. Smith Thomas, W. Thorne
         Peter, D. Woodruff Scott, and Zhang Huai-Min: Extended Reconstructed Sea Surface Temperature (ERSST), Version 4.
335   [Monthly mean SST]. NOAA National Centers for Environmental Information. doi:10.7289/V5KD1VVF. [Accessed on
         2022-11-09], 2015.
         Huang Boyin, W. Thorne Peter, F. Banzon Viva, Boyer Tim, Chepurin Gennady, H. Lawrimore Jay, J. Menne Matthew, M.
         Smith Thomas, S. Vose Russell, and Zhang Huai-Min: NOAA Extended Reconstructed Sea Surface Temperature (ERSST),
         Version 5. [Monthly mean SST]. NOAA National Centers for Environmental Information. doi:10.7289/V5T72FNM.
340   [Accessed on 2022-11-09], 2017.
         Jain, P., Castellanos-Acuna, D., Coogan, S. C. P., Abatzoglou, J. T., and Flannigan, M. D.: Observed increases in extreme
         fire weather driven by atmospheric humidity and temperature, Nature Clim., 12(1), 63-70. https://doi.org/10.1038/s41558-
         021-01224-1, 2021.
         Kalnay, E., et al.: The NCEP/NCAR 40-year reanalysis project. Bull. Am. Meteorol. Soc., 77(3), 437-471.
345   https://doi.org/10.1175/1520-0477(1996)077<0437:TNYRP>2.0.CO;2, 1996.
         Kaplan, A., Cane, M. A., Kushnir, Y., Clement, A. C., Blumenthal, M. B., and Rajagopalan, B.: Analyses of global sea
         surface temperature 1856-1991, J. Geophys. Res. Oceans, 103(C9), 18567-18589, https://doi.org/10.1029/97JC01736, 1998.
         Keeley, J. E., Brennan, T. J., and Syphard, A. D. : The effects of prolonged drought on vegetation dieback and megafires in
         southern California chaparral, Ecosphere, 13(8), e4203, https://doi.org/10.1002/ecs2.4203, 2022.
350   Koo, E., Pagni, P. J., Weise, D. R., and Woycheese, J. P.: Firebrands and spotting ignition in large-scale fires. Int. J.
         Wildland Fire, 19(7), 818-843, https://doi.org/10.1071/WF07119, 2010.
         Krawchuk, M. A., Moritz, M. A., Parisien, M. A., Van Dorn, J., and Hayhoe, K.: Global Pyrogeography: the Current and
         Future Distribution of Wildfire. PLoS One, 4(4), e5102, https://doi.org/10.1371/journal.pone.0005102, 2009.
         Kriwoken, L. K.: Australian biodiversity and marine protected areas, Ocean Coast Manag., 44(1-3), 113-132,
355   https://doi.org/10.1016/S0964-5691(96)00047-6, 1996.
         Lawson, B. D. A., OB: Weather Guide for the Canadian Forest Fire Danger Rating System, 1-84 pp., Northern Forestry
         Center, Canadian Forest Service, 2008.
         Li, X. C., Holland, D. M., Gerber, E. P., and Yoo, C.: Impacts of the north and tropical Atlantic Ocean on the Antarctic
         Peninsula and sea ice, Nature, 505(7484), 538-542, https://doi.org/10.1038/nature12945, 2014.
360   Li, X. C., Gerber, E. P., Holland, D. M., and Yoo, C.: A Rossby Wave Bridge from the Tropical Atlantic to West Antarctica,
         J. Clim., 28(6), 2256-2273, https://doi.org/10.1175/JCLI-D-14-00450.1, 2015.
         Li, X. C., Xie, S. P., Gille, S. T., and Yoo, C.: Atlantic-induced pan-tropical climate change over the past three decades.
         Nature Clim., 6(3), 275-279, https://doi.org/10.1038/nclimate2840, 2016.
         Lin, Z. D., and Li, Y.: Remote Influence of the Tropical Atlantic on the Variability and Trend in North West Australia
365   Summer Precipitation. J. Clim., 25(7), 2408-2420, https://doi.org/10.1175/JCLI-D-11-00020.1, 2012.
         Littell, J. S., Peterson, D. L., Riley, K. L., Liu, Y. Q., and Luce, C. H.: A review of the relationships between drought and
         forest fire in the United States. Global Change Biology, 22(7), 2353-2369. https://doi.org/10.1111/gcb.13275, 2016.
         Liu, D. Y., et al.: Wildfires enhance phytoplankton production in tropical oceans, Nat. Commun., 13, 1348,
         https://doi.org/10.1038/s41467-022-29013-0, 2022.
370   Liu, G. Y., Li, J., Jiang, Z. J., and Li, X. C. : Impact of Sea Surface Temperature Variability at Different Ocean Basins on
         Dust Activities in the Gobi Desert and North China, Geophys. Res. Lett., 49(15), e2022GL099821,
         https://doi.org/10.1029/2022GL099821, 2022.
         Lv, Z., Yang, J.-C., Lin, X., and Zhang, Y.: Stronger North Atlantic than Tropical Pacific Effects on North Pacific Decadal
         Prediction, J. Clim., 35(17), 5773-5785, https://doi.org/10.1175/JCLI-D-21-0957.1, 2022.

375 Mariani, M., and Fletcher, M.-S.: The Southern Annular Mode determines interannual and centennial-scale fire activity in temperate southwest Tasmania, Australia, Geophys. Res. Lett., 43(4), 1702-1709, https://doi.org/10.1002/2016GL068082, 2016.

Mariani, M., Fletcher, M. S., Holz, A., and Nyman, P.: ENSO controls interannual fire activity in southeast Australia, Geophys. Res. Lett., 43(20), 10891-10900, https://doi.org/10.1002/2016GL070572, 2016.

380 Mariani, M., Holz, A., Veblen, T. T., Williamson, G., Fletcher, M. S., and Bowman, D. M. J. S.: Climate Change Amplifications of Climate-Fire Teleconnections in the Southern Hemisphere, Geophys. Res. Lett., 45(10), 5071-5081, https://doi.org/10.1029/2018GL078294, 2018.

McGregor, S., Timmermann, A., Stuecker, M. F., England, M. H., Merrifield, M., Jin, F. F., and Chikamoto, Y.: Recent Walker circulation strengthening and Pacific cooling amplified by Atlantic warming, Nature Clim., 4(10), 888-892,
385 https://doi.org/10.1038/NCLIMATE2330, 2014.

Miller, A. J., et al.: Barotropic Rossby wave radiation from a model Gulf Stream, Geophys. Res. Lett., 34(23), L23613. https://doi.org/10.1029/2007GL031937, 2007.

Nagaraju, C., Ashok, K., Balakrishnan Nair, T. M., Guan, Z., and Cai, W.: Potential influence of the Atlantic Multi-decadal Oscillation in modulating the biennial relationship between Indian and Australian summer monsoons, Int. J. Climatol.,
390 38(14), 5220-5230. https://doi.org/10.1002/joc.5722, 2018.

Nguyen, H. D., et al.: The Summer 2019-2020 Wildfires in East Coast Australia and Their Impacts on Air Quality and Health in New South Wales, Australia, International Journal of Environmental Research and Public Health, 18(7), 3538. https://doi.org/10.3390/ijerph18073538, 2021.

Nolan, R. H., Boer, M. M., Collins, L., de Dios, V. R., Clarke, H., Jenkins, M., Kenny, B., and Bradstock, R. A.: Causes and
395 consequences of eastern Australia's 2019-20 season of mega-fires, Glob. Chang. Biol., 26(3), 1039-1041, https://doi.org/10.1111/gcb.15125, 2020.

Power, S., Casey, T., Folland, C., Colman, A., and Mehta, V.: Inter-decadal modulation of the impact of ENSO on Australia, Clim. Dyn., 15(5), 319-324, https://doi.org/10.1007/s003820050284, 1999.

Rayner, N. A., Parker, D. E., Horton, E. B., Folland, C. K., Alexander, L. V., Rowell, D. P., Kent, E. C., and Kaplan, A.:
400 Global analyses of sea surface temperature, sea ice, and night marine air temperature since the late nineteenth century. J. Geophys. Res. Atmos, 108(D14), https://doi.org/10.1029/2002JD002670, 2003.

Ren, H. C., Zuo J. Q., and Li, W. J.: The impact of tropical Atlantic SST variability on the tropical atmosphere during boreal summer, J. Clim., 34(16), 6705-6723. https://doi.org/10.1175/JCLI-D-20-0259.1, 2021.

Ren, X. Y., Zhang, L., Cai, W. J., Li, X. C., Wang, C. Y., Jin, Y. S., and Wu, L. X.: Influence of tropical Atlantic meridional
405 dipole of sea surface temperature anomalies on Antarctic autumn sea ice, Environ. Res. Lett., 17(9), 094046, https://doi.org/10.1088/1748-9326/ac8f5b, 2022.

Risbey, J. S., Pook, M. J., McIntosh, P. C., Wheeler, M. C., and Hendon, H. H.: On the Remote Drivers of Precipitation Variability in Australia. Monthly Weather Review, 137(10), 3233-3253. https://doi.org/10.1175/2009MWR2861.1, 2009.

Simpkins, G. R., McGregor, S., Taschetto, A. S., Ciasto, L. M., and England, M. H.: Tropical Connections to Climatic
410 Change in the Extratropical Southern Hemisphere: The Role of Atlantic SST Trends, J. Clim., 27(13), 4923-4936, https://doi.org/10.1175/JCLI-D-13-00615.1, 2014.

Simpson, C. C., Pearce, H. G., Sturman, A. P., and Zawar-Reza, P.: Behaviour of fire weather indices in the 2009-10 New Zealand wildland fire season, Int J Wildland Fire, 23(8), 1147-1164, https://doi.org/10.1071/wf12169, 2014.

Storch, H. v., and Zwiers, F. W.: Statistical Analysis in Climate Research, https://doi.org/10.2307/2669798, 2000
415 Trenberth, K. E.: The Definition of El Niño. Bull. Am. Meteorol. Soc., 78(12), 2771-2778. https://doi.org/10.1175/1520-0477(1997)078<2771:TDOENO>2.0.CO;2, 1997.

Trenberth, K. E., and Stepaniak, D. P.: Indices of El Niño Evolution, J. Clim., 14(8), 1697-1701, https://doi.org/10.1175/1520-0442(2001)014<1697:LIOENO>2.0.CO;2, 2001.

Trenberth, K. E., and Shea, D. J.: Atlantic hurricanes and natural variability in 2005, Geophys. Res. Lett., 33(12), L12704.
420 https://doi.org/10.1029/2006GL026894, 2006.

van der Werf, G. R., Randerson, J. T., Giglio, L., Collatz, G. J., Kasibhatla, P. S., and Arellano, A. F.: Interannual variability in global biomass burning emissions from 1997 to 2004, Atmospheric Chem. Phys., 6, 3423-3441, https://doi.org/10.5194/acp-6-3423-2006, 2006.

van Oldenborgh, G. J., et al.: Attribution of the Australian bushfire risk to anthropogenic climate change, Nat. Hazards Earth
425   Syst. Sci., 21(3), 941-960, https://doi.org/10.5194/nhess-21-941-2021, 2021.
Wang, B., Liu, J., Kim, H.-J., Webster, P. J., Yim, S.-Y., and Xiang, B.: Northern Hemisphere summer monsoon intensified
by mega-El Niño/southern oscillation and Atlantic multidecadal oscillation, Proc. Natl. Acad. Sci. U.S.A., 110(14), 5347-
5352, https://doi.org/10.1073/pnas.1219405110, 2013.
Wang, X. Y., Li, X. C., Zhu, J., and Tanajura, C. A. S. : The strengthening of Amazonian precipitation during the wet season
430   driven by tropical sea surface temperature forcing. Environ. Res. Lett., 13(9), 094015, https://doi.org/10.1088/1748-
9326/aadbb9, 2018.
Xue, J. Q., Sun, C., Li, J. P., and Mao, J. Y.: South Atlantic Forced Multidecadal Teleconnection to the Midlatitude South
Indian Ocean, Geophys. Res. Lett., 45(16), 8480-8489. https://doi.org/10.1029/2018GL078990, 2018.
Yu, P., Xu, R. B., Abramson, M. J., Li, S. S., and Guo, Y. M.: Bushfires in Australia: a serious health emergency under
435   climate change, Lancet Planet. Health, 4(1), E7-E8, https://doi.org/10.1016/S2542-5196(19)30267-0, 2020.
Zhao, S., Li, J. P., Li, Y. J., Jin, F. F., and Zheng, J. Y.: Interhemispheric influence of Indo-Pacific convection oscillation on
Southern Hemisphere precipitation through southward propagation of Rossby waves, Clim. Dyn., 52(5-6), 3203-3221,
https://doi.org/10.1007/s00382-018-4324-y, 2019.

440
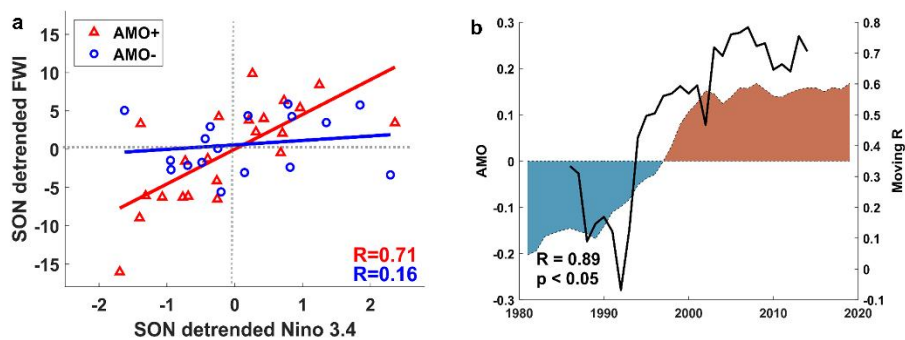
Figure 1. (a) Scatter plots for detrended, standardized SON Niño 3.4 index and the corresponding reanalysis mean Australia FWI from 1981 to 2019. The red upward triangles represent positive AMO indices, while the blue circles represent negative ones. The lines are linear fit lines. The correlation coefficient (R=0.71) corresponding to AMO+ passed the significance test of p-value<0.05, while the other one did not. **(b)** The solid black line represents the sliding correlation coefficient between

445 detrended SON FWI in Australia and detrended SON Niño 3.4 index with a sliding window of 10 years. The shaded area represents the annual AMO index. Red is positive, and blue is negative. All the correlation coefficients assume autocorrelation to the time series.
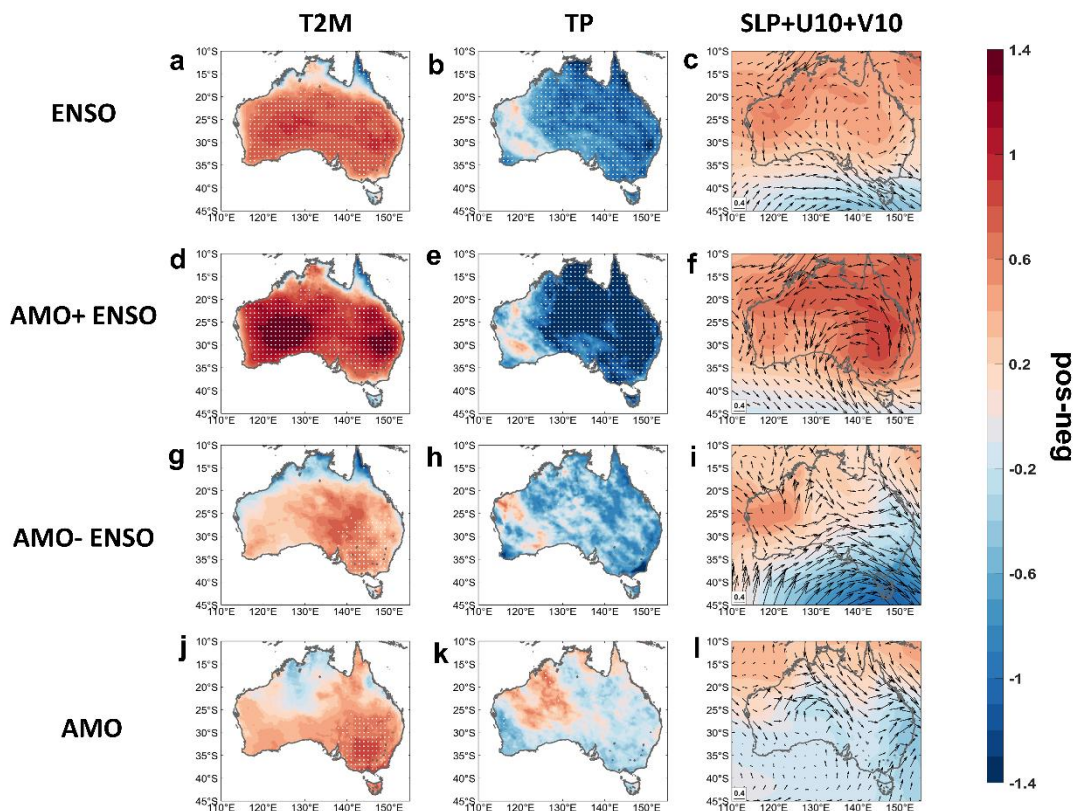
Figure 2. The difference maps for the detrended and normalized reanalysis SON **(a, d, g, j)** 2m temperature (T2M), **(b, e, h, k)** Total Precipitation (TP), and **(c, f, I, l)** Sea Level Pressure (SLP)+10m zonal and meridional winds (U10+V10) in conditions with **(a-c)** ENSO composite (El Niño composite minus La Niña composite), **(d-f)** ENSO composite with AMO+, **(g-i)** ENSO composite with AMO-, and **(j-l)** AMO composite from 1981 to 2019. The composite results are calculated using meteorological variables with positive indices minus those with negative ones. The area with white dots passed the significance test of p-value < 0.05 by Student's *t*-test.
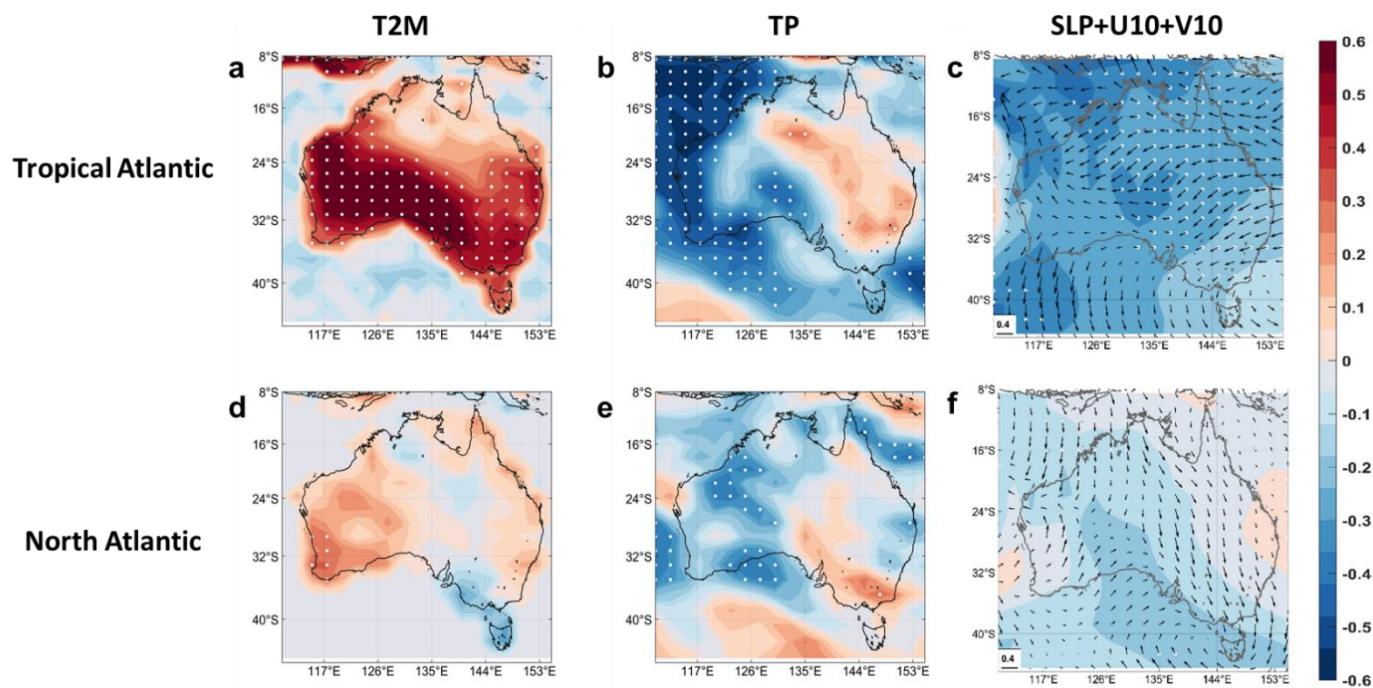
Figure 3. Regression coefficients of the ensemble mean detrended and normalized SON **(a, d)** T2M, **(b, e)** TP and **(c, f)** SLP+U10+V10 onto detrended and normalized SON **(a-c)** Tropical Atlantic (10°-60°W, 0-20°N) SST and **(d-f)** North Atlantic (10°-60°W, 25-45°N) SST in the OBE. The area with white dots passed the significance test of $p \leq 0.05$ by Student's t-test.
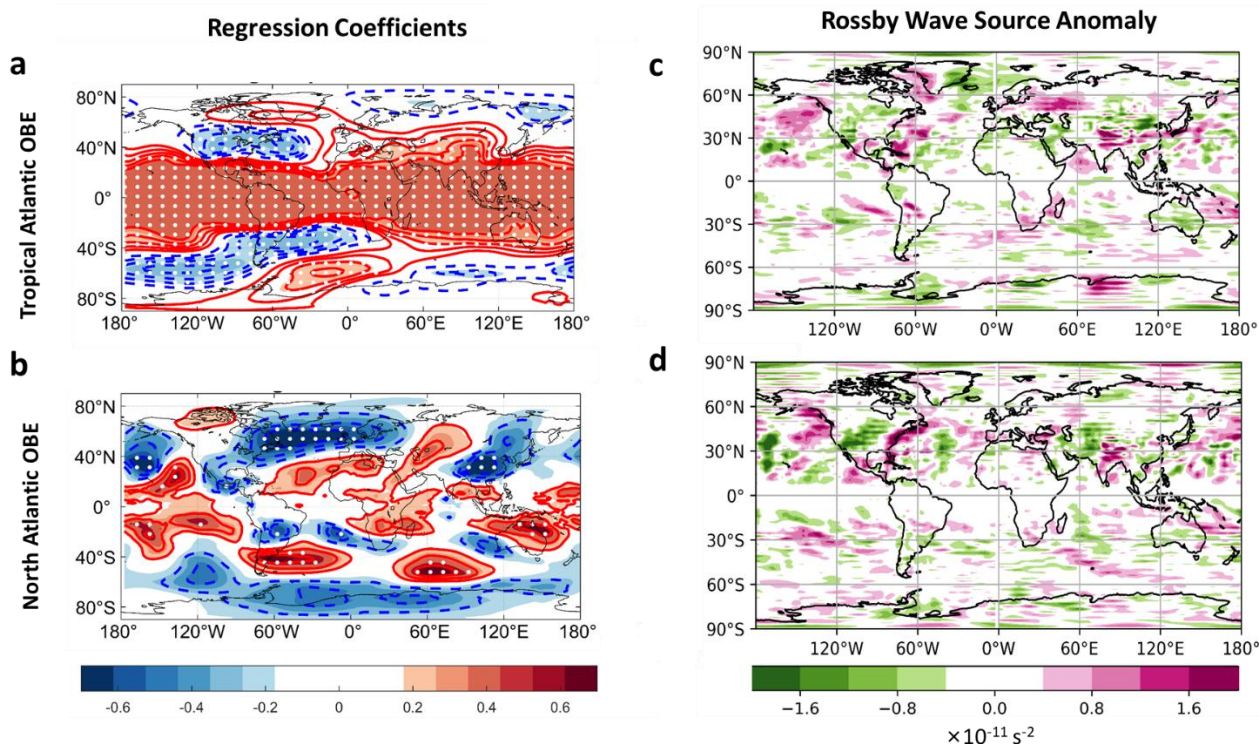
Figure 4. (a-b) Regression coefficients of detrended and normalized SON 500 hPa GPH onto detrended and normalized SON (a) Tropical Atlantic (10°-60°W, 0-20°N) and (b) North Atlantic (10°-60°W, 25-45°N) SST in the OBE. The red solid lines represent the isolines from 0.2 to 1 with an interval of 0.2, and the blue solid lines represent the isolines from - 0.2 to - 1 with an interval of - 0.2. (c-d) 200hPa Rossby wave source anomaly in (c) Tropical Atlantic OBE, and (d) North Atlantic OBE. The area with white dots passed the significance test of p ≤ 0.05 by Student's t-test.